Indian Journal of Engineering & Materials Sciences
Vol. 30, October 2023, pp. 694-699
DOI: 10.56042/ijems.v30i5.6865

Co-crystal Growth and Characterizations of Diisopropylammonium Hydrogen Phthalate

Preetika Dhawan, & Harsh Yadav*

Department of Physics, Netaji Subhas University of Technology, New Delhi 110 078, India

Received: 9 August 2023; Accepted: 26 September 2023

Slow evaporation solution growth approach has been utilized to synthesize the single co-crystal of diisopropylammonium hydrogen phthalate at room temperature. Its structural attributes owing to the refinement of its cell parameters have been successfully confirmed using Debye – Scherrer method. Ultraviolet-visible spectroscopy has further revealed the optical behaviour of the aforesaid crystal having a 301 nm cut-off with a broad direct optical energy band of 4.09 eV. Its vibrational assignments have been determined using Fourier transform infrared spectral study. Photoluminescence spectroscopy has highlighted the violet emission from the crystal when stimulated by 300 nm excitation wavelength. Vickers micro hardness technique has as certained the mechanical strength of the grown crystal along with the work-hardening coefficient thereby claiming its normal ISE behaviour to the external load. Conclusively, this work has featured the prominence of diisopropylammonium hydrogen phthalate co-crystal for optical applications.

Keywords: Co-crystal, Hardness, Photoluminescence, UV- visible optical study, XRD refinement

1 Introduction

Co-crystals aka molecule-based photo-functional materials possess exemplary features that cater to their usance in the modern technological era by virtue of their distinct physical, chemical, thermal, mechanical, opto-electrical, and even non-linear optical properties.[1]They are basically the single crystals which are prerequisite for important practical applications than their polycrystalline counterparts which possess grain boundaries thereby affecting various properties like light scattering, conductivity and even their optical behavior.[2]

Organic precursors are purposed for this study as they can easily exist in monomer or dimer forms thereby making controlled crystallization possible that can be manifested in different crystal morphologies thereby enhancing its usability in organic opto-electronics, crystal engineering avenues.[3,4]They also belong to soft category of materials and economic in value. Organic crystals offer a diverse variety of applications in photonic devices, semiconductors, superconductors, optical communication, data storage technologies due to their high optical non-linearity, chemical flexibility, wide UV transmittance etc. Organic NLO materials possess the π-bond conjugation arrangement of the molecule that is stretched across a considerable length scale and may be readily modified. The aromatic moieties are substituted with electron donor and acceptor groups, resulting in greater optical nonlinearity, optical susceptibilities, thermal stability, and electro-optic coefficient.[1,5,6]

While phthalic acid (PH) crystal on one hand possesses good mechanical stability[1] and its anhydride shows excellent properties like NLO behavior, fluorescence, phosphorescence, dendritic, spherullitic, and hollow formations etc,[5]diisopropylamine (DIPA), on the other hand, has reportedly co-crystallized into highly stable, mechanically flexible, excellent high-temperature ferroelectric[7] and NLO crystal[8–11] This research work has deliberated the supramolecular co-crystal growth of PH and DIPA moieties via controlled crystallization and re-crystallization through achieving supersaturated state using gradual evaporation at ambience temperature. This study further aims in studying and analyzing various characteristic attributes and features of the as-grown single crystal namely XRD structural refinement, UV-vis optical band gap and cut-off, photoluminescence, functional group analysis and mechanical stability following the study of various hardness parameters pertaining to several potent applications it can possess.

Furthermore, powder diffraction data has been utilized to solve the structure including indexing,

*Corresponding author (E-mail: harsh@nsut.ac.in)

space group determination and even the model refinement using Rietveld method from EXPO2014 software.[12] In addition to refinement, linear and non-linear fitting of the data have been employed to study various attributes as purposed in this study.

2 Materials and Methods

1.1 Synthesis and growth

Single co-crystals of diisopropylammonium hydrogen phthalate (DIPAPH) were as-synthesized from the saturated solution obtained by blending two precursors namely diisopropylamine (DIPA) and phthalic acid (PH) in 1:1 stoichiometric ratio in ethanol environment via the conventional slow evaporation solution growth technique (SEST) at 35.5 °C and 29% humidity.120 mm Whatman paper was utilized to occlude impurities from the prepared homogeneous solution via gravity filtration. The same was left undisturbed for about 5 months to achieve supersaturated state to trigger crystal growth. Following the timeline, highly transparent good quality crystals as long as 1.5 cm were obtained which were further subjected to different characterizations and studies. Figure 1 portrays the chemical reaction as well as the pictorial visuals of the as-grown crystals.

1.2 Characterizations

Powdered form of DIPAPH was exposed to X-rays to study its diffraction pattern (PXRD) employing RIGAKU Ultima IV, 285 diffractometer system at room temperature (Cu Kα(λ = 1.54056 A˚) X-ray source at 40kV/40mA;DivSlit-2/3 deg; DivH.L.Slit-10mm; SctSlit-2/3 deg; RecSlit-0.3mm). Furthermore, XRD refinement of its structural parameters were accomplished using EXPO2014software. Shimadzu UV-2600i spectrometer (200-800 nm) was used to trace the UV-visible transmittance pattern incorporated with single Czerny-Turner monochromator. A fluorescence spectrometer (model: QM-8450-11; 450W Xe lamp source) was used to record the photoluminescence (PL) emission spectra. DIPAPH's Fourier transform infrared (FTIR) spectra was traced on a Nicolet iS50 FTIR Tri-detector (spectrometer: Gold flex) in the 400 to 4000 cm^{-1} range using ATR method. The Vickers micro hardness technique aided in the study of hardness variation with the application of external load utilizing a diamond indenter with a 10s constant duration time and a 4s load-unload period on a Mitutoyo HM-220 machine.

3 Results and Discussion

1.3 X-ray diffraction and structural refinement

PXRD of DIPAPH was carried out in the 2θ range of 5-90° at room temperature with Cu Kα radiation (wavelength = 1.54056 Aº). Diffraction pattern so graphed in Fig. 2 reveals the peaks of (hkl) reflection properly indexed. The variety of relatively intense peaks in the XRD data validates that the grown material has a high degree of crystallinity with the highest peak pertaining to (032) plane at 22.879°, while the second highest peak corresponding to (022) plane being at 18.485° and the third highest peak corresponding to (100) plane at 10.859°. EXPO2014 software[12] was then used to optimize and refine the lattice parameters of DIPAPH, as well as to determine indexed (hkl) reflection planes and viable space groups incorporating Le Bail technique. The refined cell parameters are a=8.166097 Å, b=14.849511 Å, c=12.551641 Å, α=90°, β=93.298653°, γ=90° showing the crystal attributes to monoclinic crystal system with $P2_1$space group.

The quality of refinement has been judged via unweighted / weighted profile R factor which are R_p = 10.656, R_{wp} = 9.094. The findings are consistent with the published literature.[8]

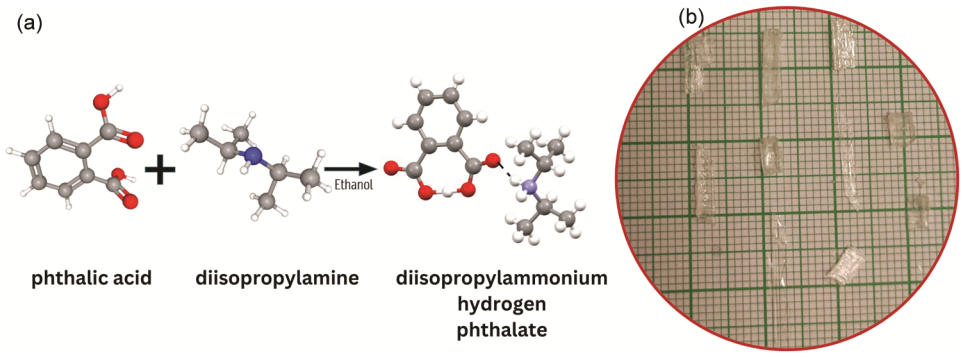

Fig. 1 — (a) Chemical reaction pertaining to co-crystal formation, and (b) Photograph of Diisopropylammonium hydrogen phthalate (DIPAPH) crystals.

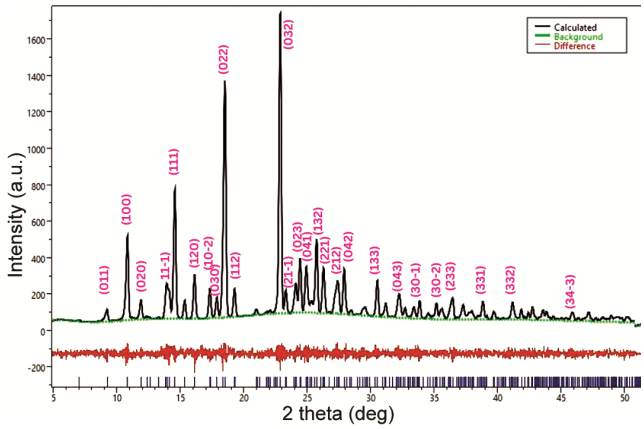

Fig. 2 — PXRD (refined) pattern of Diisopropylammonium hydrogen phthalate (DIPAPH) with indexed reflection planes.

1.4 UV-vis spectral analysis

UV-vis spectroscopy is the most often used instrument for measuring the optical characteristics, thereby deliberating the information on particle size, size distribution, aggregation stage. A crystal's UV-vis spectrum is impacted by several factors, including its thickness, optically active functional units, orientation, impurities, structural flaws, and dislocations etc.[13]

DR spectroscopy is a destructive surface examination technique that uses a mirror-like reflection from the exposed sample detected and collected by a combined spherical attachment which gives the measurement of the ratio of light scattered from a thick layer to an ideal non/weak-absorbing reference material as a function of wave length. Incident radiation on the specimen produces diffuse lighting, with incident light being partly absorbed and dispersed. According to Fig. 3, which shows the optical absorbance of the entitled crystal so obtained from the Kubelka-Munk formulation in the 200–800 nm range, the UV cut-off wavelength is reportedly 301 nm.[8] Additionally, the inset in Fig. 3 shows the Tauc plot depicting a wide and direct optical energy band gap E_g as 4.09 eV which makes it plausible for optical device applications.

1.5 Photoluminescence emission

In photoluminescence (PL) spectrum, the emission from a crystalline sample is extremely responsive to the defects existing in single crystals. In PL spectroscopy, electronic states of materials are activated by a light of specific wavelength, and the photons of varying wavelength are released pertaining to radiative recombination and because photons interact differently depending upon wavelength.[14,15]DIPAPH crystal was subjected to an

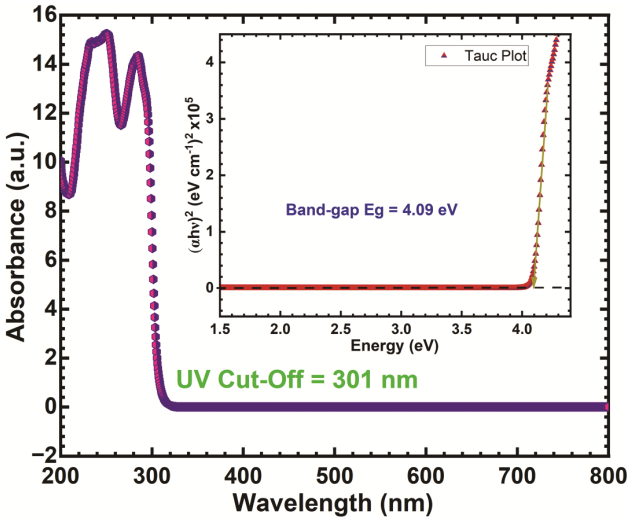

Fig. 3 — UV-vis spectrum, Inset- Tauc Plot of Diisopropylammonium hydrogen phthalate (DIPAPH)

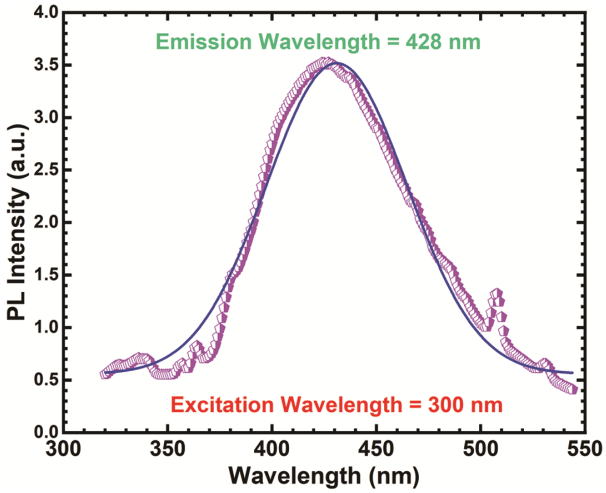

Fig. 4 — Photoluminescence spectrum of Diisopropylammonium hydrogen phthalate (DIPAPH) crystal.

excitation at 300 nm from 450W Xenon lamp source thereby leading to a peak emission at 428 nm corresponding to violet color (Fig. 4).

1.6 FTIR spectroscopy

The variety of chemical bonds present in a crystalline sample behaves differently to the input IR radiation thereby giving rise to various mode of vibrations namely stretching, bending, torsions etc[5] and helps in the determination of molecular structure, bond strength, normal modes of vibration etc.[16] The smaller broad band enveloped by peaks at 3018, 2857, 2736, 2522 cm^{-1}in Fig. 5 corresponds to the stretching vibration of O-H protonated bond thereby assuring the

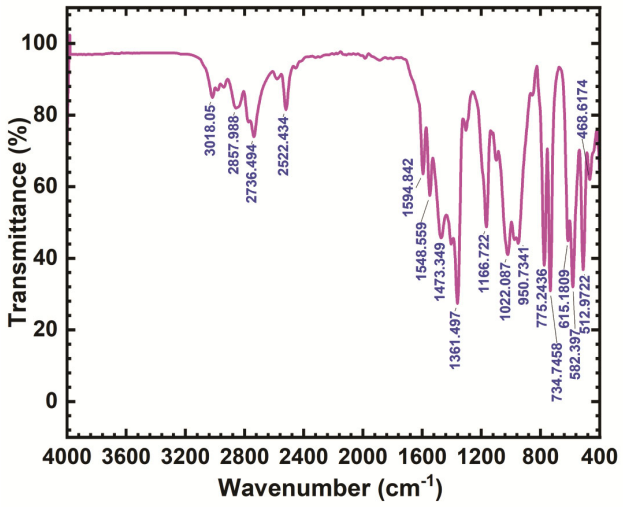

Fig. 5 — FTIR spectral analysis of Diisopropylammonium hydrogen phthalate (DIPAPH) via ATR method.

intermolecular N-H…O-H bond interaction. While 1594 cm^{-1} strong peak represents carbonyl stretching C=O vibration which is slightly varied as compared to that of phthalic anhydride crystal[5], peak at 1549 cm^{-1} represents C=C stretching in the phenyl ring.[8]N-H bending vibration is further attributed to 1473 cm^{-1}[(8)] and the stronger sharp peak at 1361 cm^{-1} is due to C-N and O-H stretching. CH-in-plane bending can be ascribed to 1361, 1167 and 1022 cm^{-1} peaks while CH-outof-plane bending can be ascribed to 951 and 775 cm^{-1} peaks.[8] C-O and C-N stretching[8]further contributes to 1167 cm^{-1} peak[8,17] and 1022 cm^{-1} pertains to the ring breathing mode of phthalate group[5,8] C-C-C bending vibrations are ascribed to 582 and 513 cm^{-1} peaks.[8]

1.7 Hardness

Mechanical attributes of a crystal play a vital role in designing and safe handling opto-electronic devices and in manufacturing pharmaceutical materials by virtue of improving powder handling and its integrity.[1,18] A material's hardness narrates its resistance to the local deformation subjected to it via indenting it through pyramidal diamond indenter pertaining to Vickers microhardness method.[19] This in a way is affected by the motion of dislocations due to impurities within the crystal lattice and even by the presence of defects.[18]Vickers microhardness number (H_v; kg/ mm^2; MPa) was calculated from the formula H_v=1.8544 P/d^2(kg/mm^2) = 0.1891 F/d^2(N/mm^2 = MPa), where d is the average length along two diagonals of the indent (mm) and P is the load of the applied indentation (kg) (aka force F in N). Figure. 6 is a recapitulation of all the studied hardness parameters namely (a) 50X optical images of the indentation marks, (b) microhardness analysis with varying P, study of (c) Meyer's law, (d) Hays and Kendall's technique and (e) proportional specimen resistance (PSR).Crystal exhibited reverse ISE (RISE) behaviour throughout a relatively short load range, with a maximum at P_m = 3g. This may be resulted because of the presence of zone distortion at the interface of crystal and medium or due to the vibration, low load indenter bluntness, specimen chipping, crack formation during indenter loading etc. Post P_m =3g, for a considerable higher range, crystal showed normal ISE behavior. This normal ISE behavior corresponds to numerous factors including work hardening amid indentation, initiation of plastic deformity while loading, indentation elastic recovery, combination of elastic/plastic deformity response of crystal, etc. Crystal tore apart when P= 200g was applied. Next, according to Meyer's law which was used to explain the normal ISE conduct that holds a significant contribution; $P = Ad^n$; n = Meyer's index; A is a geometric conversion factor of the pyramidal indenter. Graph was analyzed in two sections low and high load region pertaining to the abrupt transitioning at P_m. For low load region, n = 2.92 depicting RISE behavior and for high load region, n=1.59 depicting ISE behavior as prescribed.[20,21]n=1.76 and A = 22.33 x 10^{-3}g/µm for the entire load fitted graph describing the major contribution of ISE behavior showing that the DIPAPH belongs to soft category.[1,20,21] In Hays and Kendall's approach, load dependence of hardness $P = W + Bd^2$; W is the limited load to initiate plastic deformity and B is a load-independent constant. W = 0.43 g and B = 0.009 g/µm^2 = 9 kg /mm^2 (for the whole range fitting). PSR model is further attributed to normal ISE behavior described by the relation $P = ad + bd^2$ where the parameter a characterizes the load dependence of hardness and b is a load-independent constant. a = 0.13 g/µm, b = 0.006 g/µm^2 for ISE behavior in high load region while a = -0.13 g/µm, b = 0.02 g/µm^2 for RISE behavior in low load region. Critical indentation diagonal d_c = 13.34 µm corresponds to P_m. It was further noticed that the residual stress, defined as the ratio of a and b, increased in high load region. Formation of cracks and plastic deformity are mainly responsible for sudden breaks owing to distinct slopes a/b at low and high loads.[20,21]

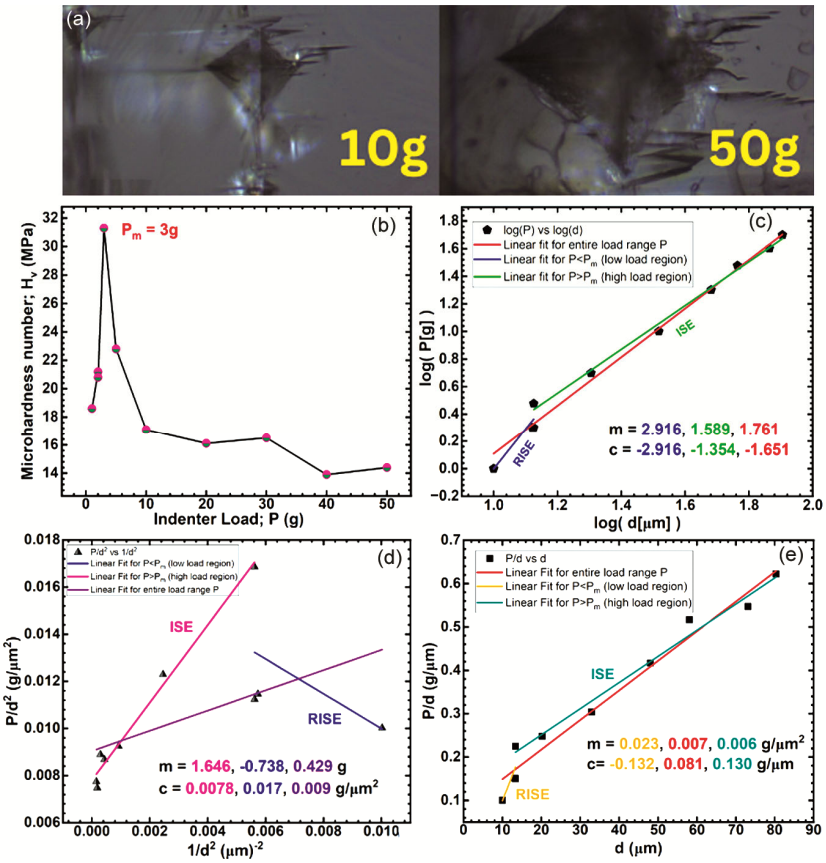

Fig. 6 — (a) 50X optical indentation images, Variation of (b) micro hardness with applied load, (c) log P with log d, (d) P/d^2 with $1/d^2$, & (e) P/d with d.

4 Conclusion

This article sketches a brief elaboration of the successful solution development of good-quality, good-sized single crystals of DIPAPH. Powder XRD pattern along with refinement done has surely confirmed the development and cell characteristics of the crystal, thus demonstrating that it is in accordance with the monoclinic system of crystals with $P2_1$ space group. Furthermore, the crystal has possessed broader optical band gap with UV-vis cut-off at 301 nm. When stimulated by a 300 nm excitation source, the PL spectroscopy has detected a violet emission peak at 428 nm. Functional groups have been further ascertained thereby validating the intermolecular hydrogen bonding interaction N–H…O. Hardness studies has reported that DIPAPH possesses a good mechanical strength and depicts normal indentation size effect. The inference is thus drawn out claiming DIPAPH a potential candidate for photonic applications.

Acknowledgement

Preetika Dhawan is highly grateful for sincere supervision and guidance of Dr. Harsh Yadav, Assistant Professor, Netaji Subhas University of Technology, Dwarka, Delhi. They both are highly indebted to the Vice Chancellor, NSUT, Delhi for sponsoring this work.

References

1 Kumar M S, Rajesh K, Vijayaraghavan G V, Krishnan S, *Mater Res Express*, 5 (2018).
2 Bhat H L, *Introduction to crystal growth: principles and practice* (CRC Press, Florida) 2015.
3 Sun Y, Tilbury C J, Reutzel-Edens S M, Bhardwaj R M, Li J, Doherty M F, *Cryst Growth Des*, 18 (2018) 905.
4 Ehmann H M A, Werzer O, *Cryst Growth Des*, 14 (2014) 3680.
5 Janarthanan S, Rajan Y C, Samuel R S, Pandi S, Adv *Mat Res,* 584 (2012) 136.
6 Prince S, Suthan T, Gnanasambandam C, J *Electron Mater*, 51 (2022) 1639.
7 Fu D W, Cai H L, Liu Y, Ye Q, Zhang W, Zhang Y, Chen X Y, Giovannetti G, Capone M, Li J, Xiong R G, *Science*, 339 (2013) 425.
8 Gino D J, Sidden C, Paulraj R, Ajitha S, Somaily H H, *J Mater Sci Mater Electron*, 33 (2022) 16923.
9 Vij M, Sonia, Yadav H, Vashistha N, Kumar P, Maurya K K, J *Mol Struct*, 1206 (2020).
10 Vij M, Yadav H, Goel S, Vashisthaa N, Sonia, Nayaka D, Kumar P, Maurya K K, *J MolStruct,*1246 (2021) 131177.

11 Dhawan P, Saini A, Goel S, Tyagi N, Yadav H, *J Mol Struct*, 1270 (2022).
12 Altomare A, Cuocci C, Giacovazzo C, Moliterni A, Rizzi R, Corriero N and Falcicchio A*, J Appl Cryst*, 46 (2013) 1231.
13 Phan V T, Do T T P, Nguyen D T, Nguyen K D, Vo T T N, Le A T Q, Huynh D T, *Opt Quantum Electron*, 53 (2021).
14 Vij M, Yadav H, Vashistha N, Kumari M, Verma H K, Kumar P, Maurya K K, *J Mater Sci*, 55 (2020) 16900.
15 Inkrataite G, Laurinavicius G, Enseling D, Zarkov A, Jüstel T, Skaudzius R, Crystals *(Basel)*, 11 (2021).
16 Reena Priya J, Mercina M, Nancy M P, Mary Linet J, Arul Martin Mani J, *Mater Today Proc*, 65 (2022) 385.
17 Thangavel P, Karuppanan S, Muthusamy Poomalai P, Sakthivel A, Nandagopalan G, Bellucci S, Photonics, 9 (2022).
18 Liu F, Hooks D E, Li N, Rubinson J F, Wacker J N, Swift J A, *Chemistry of Materials*, 32 (2020) 3952.
19 Fernandes J M, Mahendra K, Udayashankar N K, *Opt Mater (Amst)*, 110 (2020).
20 Farhat, S., Rekaby, M. &Awad, *SN ApplSci,* 1 (2019)546.
21 Goel S, Sinha N, Yadav H, Hussain A, Kumar B,*Mater Res Bult,*83 (2016) 77.